Egypt. J. Chem. **Vol. 66**, No. 10 pp. 603 - 620 (2023)

Egyptian Journal of Chemistry

http://ejchem.journals.ekb.eg/

New Fluorinated Pyrazolo [1,5-*A*]Pyrimidines As Potential Anticancer Agents: Synthesis, Anticancer Evaluation, Molecular Docking Simulation and ADME Study

Mona Said Mohamed[a], Zinab Atwa Saad[a] and Nadia Hanafy Metwally[a,*]

[a]*Chemistry Department, Faculty of Science, Cairo University, Giza 12613, Egypt*

Abstract

The new starting compounds **5a,b** 2-(cyanomethyl)-7-(4-fluorophenyl)-5-(heteroyl-2-yl)pyrazolo[1,5-*a*]pyrimidine-3-carbonitrile, which prepared from *α,β*-unsaturated carbonyl compounds with 5-amino-3-cyanomethyl-1*H*-pyrazole-4-carbonitrile (**4**) was reacted with each of aromatic aldehydes, and arenediazonium salts to yield a series of novel fluorinated pyrazolo[1,5-*a*]pyrimidine derivatives. All the new compounds prepared were supported *via* spectroscopic tools and elemental analyses. The anticancer activity of some selected compounds was examined in *vitro* against three lines. Among the other prepared compounds, **7i-l** are appeared anticancer activity among the other prepared compounds, additionally, compound **7i** is more potent anticancer compound of IC_{50} = 7.84± 0.6, 5.63± 0.4 and 3.71± 0.1 µg/ml against HepG2, MCF7 and HeLa, respectively. Further, using the molecular docking MOE 2014.10 software, compounds **7i, 7j** and **7k** were docked with the active site of the 1Y8Y enzyme. The results indicated that there are good hydrogen bond interactions between the target compounds and the Lys 129, lys 89, Lys 33, Asp 89, Gly 8, Gly 13, residues in terms of bond lengths and binding energies. Moreover, ADME study was performed for the selected potent anticancer compounds.

Keywords: fluorinated pyrazolo[1,5-*a*]pyrimidines, anticancer activity, molecular docking and ADME studies.

1. Introduction

According to the WHO, nearly 10 million people died from cancer in 2020, with lung cancer (1.80 million deaths), colon and rectum (916000 million deaths), liver (830000 million deaths) and breast (685000 million deaths) being the most common. These numbers are still increasing due to the lack of efficient and selective anticancer medicines. There an urgent need to focus on the design, synthesis, and production of more potent and effective human therapeutics to treat cancer disease, the leading cause of death worldwide [1]. Pyrazolo[1,5-*a*]pyrimidines, as purine analogues are of great interest in medicinal chemistry [2]. Furthermore, there are several drugs with pyrazolo[1,5-a]pyrimidine as their core showed promise different activities [3-6]. For example,

*Corresponding author e-mail: mnadia@sci.cu.edu.eg.; (Nadia Hanafy Metwally).
EJCHEM use only: Received date 24 January 2023; revised date 09 July 2023; accepted date 13 February 2023
DOI: 10.21608/EJCHEM.2023.189503.7505

indiplon is used to treat insomnia and depression drug (Fig. 1). Zaleplon is a sedative hypnotic used to treat insomnia (Fig. 1). In addition, there is ocinaplon used as an anxiolytic, and anagliptin, used to treat type 2 diabetes (Fig. 1). In the last two decades, there is a growing interest in the synthesis of pyrazolo[1,5-*a*]-pyrimidine derivatives as promising drugs for treatment of cancer diseases. For example, dinaciclib has been synthesized as a potent and selective cyclin-dependent kinase (CDK) inhibitor and is currently under clinical evaluation (Fig. 1) [7].

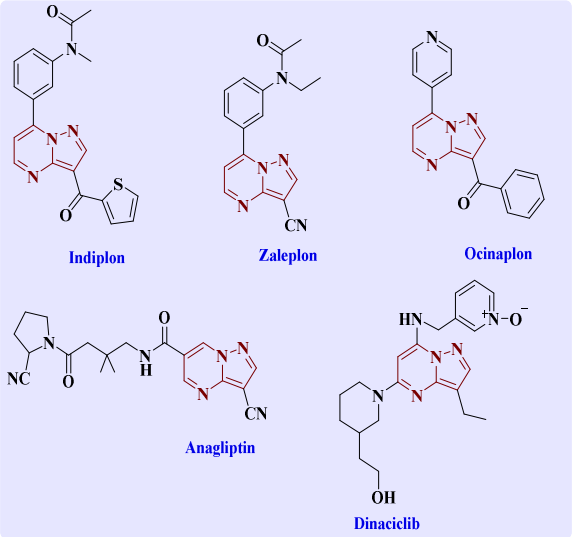

Figure 1: Some drugs contained pyrazolo[1,5-*a*]-pyrimidine core

It have been reported that remarkable electronic, physical, biological properties and reactivity of fluoro-organic compounds, as compared with those of non-fluorinated counterparts, are being commonly used for technological innovations such as a new substituted pyrazolo[1,5-*a*]pyrimidine **I** was active against HeLa cell lines, with respective IC_{50} value appear below 10 µM better than cisplatin a market drug, as shown in Fig. 2 [8]. Additionally, dacomitinib (Vizimpro) **II**, a selective and irreversible inhibitor of EGFR, which was approved in 2018, by the FDA for the treatment of non-small cell lung cancer (Fig. 2) [9].

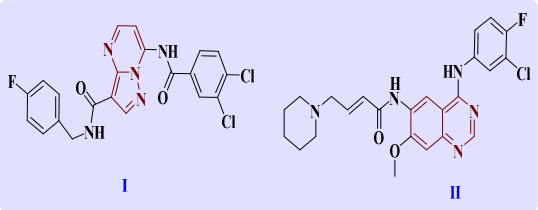

Figure 2: Fluorinated compounds as anticancer drugs

On the basis of these findings and the anticancer structures **I**, **II** and on our continuing interest in the synthesis of some new bioactive heterocyclic compounds, [10-19] we hereby report new heterocycles based on pyrimidine, pyrazole, and fluorine structural units starting from the previously unreported hitherto 2-(cyanomethyl)-7-(heteryl-2-yl)-5-fluoropyrazolo[1,5-*a*]pyrimidine-3-carbonitriles, then evaluate their anticancer actively.

2. Experimental

All melting points were determined on an Electrothermal (9100) apparatus and are uncorrected. The IR spectra were recorded as KBr pellets on a Perkin Elmer 1430 spectrophotometer. The NMR spectra were recorded with a Varian Mercury VXR-300 NMR spectrometer at 300 and 75 MHz (^{1}H and ^{13}C NMR spectra, respectively) using DMSO-*d*6 as solvents and results are expressed as δ values. Mass spectra were taken on a Shimadzu GCMS-QP 1000 Ex mass spectrometer at 70 eV. Elemental analyses were carried out at the Microanalyses Center at Cairo University and were performed on Vario EL III Elemental CHNS analyzer. The anticancer activity was carried out in faculty of pharmacy at Egypt's Mansoura University. Enzyme inhibition, cell cycle and apoptosis were performed at VACSERA, Cairo, Egypt.

Synthesis of 3-(4-fluorophenyl)-1-(heteroyl-2-yl)prop-2-en-1-one ***(3a,b)***

A solution of 4-fluorobenzaldehyde (**1**) (2 mmol) and appropriate methyl ketones (**2a,b**) (2 mmol) in 10 mL of absolute ethanol was stirred together for 10 minutes then 6 mL of 20% KOH was added dropwise, stirring was completed to 24h. The mixture was poured into crushed ice and acidified with ice-cold hydrochloric acid. The product obtained was filtered, washed with water, and dried.

3-(4-Fluorophenyl)-1-(thiophen-2-yl)prop-2-en-1-one **(3a).**
Yellow crystals; yield 94%; m.p.120 °C [20]; IR (KBr) ν_{max} / cm^{-1} = 1590 (C=C), 1644 (CO); ^{1}H NMR (DMSO) δ = 7.20 (d, 1H, *J* = 15 Hz, =CH)**,** 7.23-7.27(m, 1H, thiophene), 7.38-7.87 (m, 4H , Ar), 7.64 (d, 1H, *J* = 15 Hz, =CH)**,** 7.98-8.13 (m, 2H, thiophene); Anal. Calcd $C_{13}H_9FOS$ (232.04): C, 67.22; H, 3.91; F, 8.18; S, 13.80. Found: C, 67.38; H, 3.71; S, 13.94%.

3-(4-Fluorophenyl)-1-(furan-2-yl)prop-2-en-1-one **(3b).**
Yellow crystals; yield 94%; m.p. 110 °C [21]; IR (KBr) ν_{max} / cm^{-1} = 1601(C=C), 1660 (CO); ^{1}H NMR (DMSO) δ = 7.17 (d, 1H, *J* = 15 Hz, =CH), 7.45-7.89 (m, 4H , Ar),7.59 (d, 1H, *J* = 15 Hz, =CH), 7.91-8.02 (m, 3H, furan); Anal. Calcd $C_{13}H_9FO_2$ (216.06): C, 72.22; H, 4.20; F, 8.79. Found: C, 72.09; H, 4.31%.

*Synthesis for compounds **5a,b**.*
Equimolar amounts of 5-amino-3-(cyanomethyl)-1*H*-pyrazole-4-carbonitrile (**4**) were heated with 3-(4-fluorophenyl)-)prop-2-en-1-one derivatives (**3a,b**) under reflux in sodium ethoxide solution for 5-6 h. Solid product was filtered off, washed with ethanol, and recrystallized from ethanol-dioxane mixture.

2-(Cyanomethyl)-7-(4-fluorophenyl)-5-(thiophen-2-yl)pyrazolo[1,5-*a*]pyrimidine-3-carbonitrile **(5a).**
Dark brown crystals; yield 74%; m.p. > 300 °C; IR (KBr) ν_{max} / cm^{-1} = 2218 (CN); ^{1}H NMR (DMSO) δ = 3.77 (s, 2H, CH_2), 7.03-7.25 (m, 1H, thiophene), 7.52 (d, 2H, *J* = 8.4, Ar), 7.73 (d, 1H, *J* = 4.8 Hz, thiophene), 7.82 (d, 2H, *J* = 8.4, Ar), 7.98-8.03 (d, 1H , *J* = 4.8 Hz, thiophene), 8.29 (s, 1H, pyrimidin); Anal. Calcd for $C_{19}H_{10}FN_5S$: C, 63.50; H, 2.80; F, 5.29; N, 19.49; S, 8.92. Found: C, 63.38; H, 2.93; N, 19.33; S, 8.81%.

2-(Cyanomethyl)-7-(4-fluorophenyl)-5-(furan-2-yl)pyrazolo[1,5-*a*]pyrimidine-3-carbonitrile **(5b).**
Dark brown crystals; yield 65%; m.p. > 300 °C; IR (KBr) ν_{max} / cm^{-1} = 2212 (CN); ^{1}H NMR (DMSO) δ = 3.53 (s, 2H, CH_2), 7.11-7.24 (m, 1H, furan), 7.41 (d, 2H, *J* = 8.4, Ar), 7.59 (d, 1H, *J* = 5 Hz, furan), 7.68 (d, 2H, *J* = 8.5, Ar), 7.86 (d, 1H, *J* = 5 Hz, furan), 8.27(s, 1H, pyrimidin); Anal. Calcd for $C_{19}H_{10}FN_5O$: C, 66.47; H, 2.94; F, 5.53; N, 20.40. Found: C, 66.34; H, 2.81; N, 20.53%.

Synthesis of compounds **7a-l.**
(5 mmol) of 2-(cyanomethyl)-7-(4-fluorophenyl)-5-substituted pyrazolo[1,5-*a*]pyrimidine-3-carbonitriles **5a,b** and (5 mmol) of aromatic aldehydes (**6a-l**) were refluxed in DMF containing piperidine as a basic catalyst for 5-6 h. The precipitate was filtered off, washed with ethanol and recrystallized from ethanol-dioxane mixture.

2-(1-Cyano-2-phenylvinyl)-7-(4-fluorophenyl)-5-(thiophen-2-yl)pyrazolo[1,5-*a*]pyrimidine-3-carbonitrile **(7a).**
Dark brown crystals; yield 85%; m.p. > 300 °C; IR (KBr) ν_{max} / cm^{-1} = 2214 (CN) ;^{1}H NMR (DMSO) δ = 7.01-7.20 (m, 1H, thiophene), 7.37-7.54 (m, 5H, Ar), 7.38 (d, 2H, *J* = 8.5, Ar), 7.62 (d, 1H , *J* = 4.5 Hz, thiophene), 7.72 (d, 2H, *J* = 8.5, Ar), 7.89 (d, 1H , *J* = 4.8 Hz, thiophene), 8.22 (s, 1H, pyrimidin), 8.36 (s, 1H, CH); Anal. Calcd for $C_{26}H_{14}FN_5S$ (447.49): C,

69.79; H, 3.15; F, 4.25; N, 15.65; S, 7.16. Found: C, 69.52; H, 3.32; N, 15.82; S, 7.02%.

2-(1-Cyano-2-(4-methoxyphenyl)vinyl)-7-(4-fluorophenyl)-5-(thiophen-2-yl)pyrazolo[1,5-*a*]pyrimidine-3-carbonitrile **(7b).**
Dark brown crystals; yield 70%; m.p. > 300 °C; IR (KBr) ν_{max} / cm^{-1} = 2219 (CN) ; ^{1}H NMR (DMSO) δ = 3.80 (s, 3H, OCH_3), 7.15-7.59 (m, 4H, Ar), 7.33 (d, 2H, *J* = 8.5, Ar), 7.61-7.89 (m, 2H, thiophene), 7.75 (d, 2H, *J* = 8.4, Ar), 7.93 (d, 1H , *J* = 4.8 Hz, thiophene), 8.23 (s, 1H, pyrimidin), 8.47 (s, 1H, CH); ^{13}C NMR (DMSO) δ = 59.73, 102.54, 113.53, 116,72, 116.82, 117, 126.30, 128.45 130.22, 133.51, 136.71, 141.25, 146.63, 152.66, 156.72, 159.69, 162.78, 166.84; Anal. Calcd for $C_{27}H_{16}FN_5OS$ (477.52): C, 67.91; H, 3.38; F, 3.98; N, 14.67; S, 6.71;. Found: C, 67.75; H, 3.55; N, 14.53; S, 6.59%.

2-(1-Cyano-2-(2,5-dimethoxyphenyl)vinyl)-7-(4-fluorophenyl)-5-(thiophen-2-yl)pyrazolo[1,5-*a*]pyrimidine-3-carbonitrile **(7c).**
Dark brown crystals; yield 70%; m.p. > 300 °C; IR (KBr) ν_{max} / cm^{-1} = 2213 (CN); ^{1}H NMR (DMSO) δ = 3.65 (s, 3H, OCH_3), 3.72 (s, 3H, OCH_3), 6.82-6.97 (m, 3H, Ar), 7.25-7.36 (m, 2H, thiophene), 7.39-7.85 (m, 4H, Ar), 7.92 (d, 1H , *J* = 5 Hz, thiophene), 8.32 (s, 1H, pyrimidin), 8.49 (s, 1H, CH); ^{13}C NMR (DMSO) δ = 57.22, 59.62, 102.64, 110.63, 113.62, , 114.89, 116.72, 116.94, 117.41, 126.64, 129.85, 130.26, 133.14, 139.51, 140.35, 152.66, 155.16, 159.26, 160.43, 166.72. Anal. Calcd. for $C_{28}H_{18}FN_5O_2S$ (507.54): C, 66.26; H, 3.57; F, 3.74; N, 13.80; S, 6.32; Found: C, 66.44; H, 3.63; N, 13.66; S, 6.48%.

2-(1-Cyano-2-(4-hydroxy-3-methoxyphenyl)vinyl)-7-(4-fluorophenyl)-5-(thiophen-2-yl)pyrazolo[1,5-*a*]pyrimidine-3-carbonitrile **(7d).**
Dark brown crystals; yield 65%; m.p. >300 °C; IR (KBr) ν_{max} / cm^{-1} = 3433 (OH), 2218 (CN); ^{1}H NMR (DMSO) δ = 3.54 (s, 3H, OCH_3), 7.02-7.25 (m, 3H, Ar), 7.27-7.32 (m, 2H, thiophene), 7.34-7.83(m, 4H, Ar), 7.97 (d, 1H , *J* = 5.2 Hz, thiophene), 8.24 (s, 1H, pyrimidin), 8.40(s, 1H, CH), 10.32 (s, 1H, OH); Anal. Calcd for $C_{27}H_{16}FN_5O_2S$ (493.52): C, 65.71; H, 3.27; F, 3.85; N, 14.19; S, 6.50. Found: C, 65.87; H, 3.12; N, 14.02; S, 6.39%.

2-(1-Cyano-2-(furan-2-yl)vinyl)-7-(4-fluorophenyl)-5-(thiophen-2-yl)pyrazolo[1,5-*a*]pyrimidine-3-carbonitrile **(7e).**
Dark brown crystals; yield 70%; m.p. > 300 °C; IR (KBr) ν_{max} / cm^{-1} = 2213 (CN); ^{1}H NMR (DMSO) δ = 7.02 -7.28 (m, 3H, furan), 7.33-7.78 (m, 4H, Ar), 7.69-7.82 (m, 2H, thiophene), 7.98 (d, 1H, *J* = 5 Hz, thiophene), 8.20 (s, 1H, pyrimidin), 8.43 (s, 1H, CH); Anal. Calcd for $C_{24}H_{12}FN_5OS$ (437.45): C, 65.90; H, 2.77; F, 4.34; N, 16.01; S, 7.33. Found: C, 65.75; H, 2.64; N, 16.18; S, 7.21%.

2-(1-Cyano-2-(thiophen-2-yl)vinyl)-7-(4-fluorophenyl)-5-(thiophen-2-yl)pyrazolo[1,5-*a*]pyrimidine-3-carbonitrile **(7f).**
Dark brown crystals; yield 65%; m.p. > 300 °C; IR (KBr) ν_{max} / cm^{-1} = 2215 (CN); ^{1}H NMR (DMSO) δ = 7.16-7.52 (m, 3H, thiophene), 7.38-7.41 (m, 2H, thiophene), 7.79-7.82 (m, 4H, Ar), 7.89 (d, 1H , *J* = 4.9 Hz, thiophene), 8.02 (s, 1H, pyrimidin), 8.25 (s, 1H, CH); Anal. Calcd for $C_{24}H_{12}FN_5S_2$ (453.51): C, 63.56; H, 2.67; F, 4.19; N, 15.44; S, 14.14; Found: C, 63.42; H, 2.82; N, 15.31; S, 14.02. %

2-(1-Cyano-2-phenylvinyl)-7-(4-fluorophenyl)-5-(furan-2-yl)pyrazolo[1,5-*a*]pyrimidine-3-carbonitrile **(7g).**
Dark brown crystals; yield 75%; m.p. > 300 °C; IR (KBr) ν_{max} / cm^{-1} = 2212 (CN); ^{1}H NMR (DMSO) δ = 7.26-7.58 (m, 5H, Ar), 7.61-7.73 (m, 2H, furan), 7.83-7.86 (m, 4H, Ar), 7.92 (d, 1H , *J* = 4.8 Hz, furan), 8.20 (s, 1H, pyrimidin), 8.41(s, 1H, CH);

Anal. Calcd for $C_{26}H_{14}FN_5O$ (431.43): C, 72.38; H, 3.27; F, 4.40; N, 16.23; Found: C, 72.49; H, 3.15; N, 16.37%.

2-(1-Cyano-2-(4-methoxyphenyl) vinyl)-7-(4-fluorophenyl)-5-(furan-2-yl)pyrazolo[1,5-*a*]pyrimidine-3-carbonitrile **(7h).**
Dark brown crystals; yield 70%; m.p. > 300 °C; IR (KBr) ν_{max} / cm^{-1} = 2213 (CN); ^{1}H NMR (DMSO) δ = 3.77 (s, 3H, OCH_3), 7.02-7.49 (m, 2H, furan), 7.26-7.65 (m, 4H, Ar), 7.33 -7.75 (m, 4H, Ar), 7.94 (d, 1H , *J* = 5.3 Hz, furan), 8.07 (s, 1H, pyrimidin),8.42 (s, 1H, CH); Anal. Calcd for $C_{27}H_{16}FN_5O_2$ (461.46): C, 70.28; H, 3.50; F, 4.12; N, 15.18. Found: C, 70.43; H, 3.38; N, 15.24%.

2-(1-Cyano-2-(2,5-dimethoxyphenyl)vinyl)-7-(4-fluorophenyl)-5-(furan-2-yl)pyrazolo[1,5-*a*]pyrimidine-3-carbonitrile **(7i).**
Dark brown crystals; yield 80%; m.p. > 300 °C; IR (KBr) ν_{max} / cm^{-1} = 2211 (CN); ^{1}H NMR (DMSO) δ = 3.52 (s, 3H, OCH_3), 3.74 (s, 3H, OCH_3), 7.01-7.15 (m, 3H, Ar), 7.22-7.28 (m, 2H, furan), 7.36-7.81 (m, 4H, Ar), 7.98 (d, 1H , *J* = 5.2 Hz, furan), 8.16 (s, 1H, pyrimidin), 8.40 (s, 1H, CH); Anal. Calcd for $C_{28}H_{18}FN_5O_3$ (491.48): C, 68.43; H, 3.69; F, 3.87; N, 14.25. Found: C, 68.29; H, 3.57; N, 14.12%.

2-(1-Cyano-2-(4-hydroxy-3-methoxyphenyl)vinyl)-7-(4-fluorophenyl)-5-(furan-2-yl)pyrazolo-[1,5-*a*]pyrimidine-3-carbonitrile **(7j).**
Dark brown crystals; yield 85%; m.p. > 300 °C; IR (KBr) ν_{max} / cm^{-1} = 3443 (OH), 2218 (CN); ^{1}H NMR (DMSO) δ = 3.74 (s, 3H, OCH_3), 7.05-7.19 (m, 3H, Ar), 7.31-7.36 (m, 2H, furan), 7.39-7.84 (m, 4H, Ar), 7.99 (d, 1H , *J* =5 Hz, furan), 8.01 (s, 1H, pyrimidin), 8.46 (s, 1H, CH), 10.24 (s, 1H, OH); ^{13}C NMR (DMSO) δ = 59.42, 103.44, 110.21, 114.87, 116.41, 116.59, 117.29, 128.40, 130.06, 133.54, 138.90, 139.30, 140.53, 145.63, 149.56, 152.22, 164.84, 155.07, 160.31, 166.74; Anal. Calcd for $C_{27}H_{16}FN_5O_3$ (477.46): C, 67.92; H, 3.38; F, 3.98; N, 14.67. Found: C, 67.78; H, 3.25;N, 14.82%.

2-(1-Cyano-2-(furan-2-yl)vinyl)-7-(4-fluorophenyl)-5-(furan-2-yl)pyrazolo[1,5-*a*]pyrimidine-3-carbonitrile **(7k).**
Dark brown crystals; yield 70%; m.p. > 300 °C; IR (KBr) ν_{max} / cm^{-1} = 2216 (CN); ^{1}H NMR (DMSO) δ = 6.98-7.32 (m, 2H, furan), 7.34-7.37 (m, 2H, furan), 7.39-7.88 (m, 4H, Ar), 7.93 (d, 2H , *J* = 5 Hz, furan), 8.07 (s, 1H, pyrimidin), 8.42 (s, 1H, CH); Anal. Calcd for $C_{24}H_{12}FN_5O_2$ (421.39): C, 68.41; H, 2.87; F, 4.51; N, 16.62. Found: C, 68.29; H, 2.75; N, 16.85%.

2-(1-Cyano-2-(thiophen-2-yl)vinyl)-7-(4-fluorophenyl)-5-(furan-2-yl)pyrazolo[1,5-*a*]pyrimidine-3-carbonitrile **(7l).**
Dark brown crystals; yield 80%; m.p. > 300 °C; IR (KBr) ν_{max} / cm^{-1} = 2213 (CN); ^{1}H NMR (DMSO) δ = 6.89-6.93 (m, 1H, thiophene), 7.32-7.41 (m, 2H, thiophene), 7.33-7.36 (m, 2H, furan), 7.39-7.87 (m, 4H, Ar), 7.94 (d, 1H , *J* = 5.2 Hz, furan), 8.07 (s, 1H, pyrimidin), 8.16 (s, 1H,CH); Anal. Calcd for $C_{24}H_{12}FN_5OS$ (437.45): C, 65.90; H, 2.77; F, 4.34; N, 16.01; S, 7.33. Found: C, 65.75; H, 2.93; N, 16.23; S, 7.19%.

Synt*hesis of compounds* **9a-e.**
Diazonium salt of aromatic amines **8a-e** was prepared by diazotizing the corresponding aromatic amines (2.5 mmol) in concentrated hydrochloric acid with sodium nitrite (2.65 mmol) was added to cold solution of **5a,b** (0.5 g, 2.5 mmol) in pyridine (2.5 mmol). The addition was carried out drop wise with stirring at 0-5 °C. After complete addition and stirring in ice for few minutes, the solid formed was collected by filtration, washed with water, dried, and recrystallized from ethanol-dioxane mixture to give compounds **9a-e**.

3-Cyano-7-(4-fluorophenyl)-*N*-phenyl-5-(thiophen-2-yl)pyrazolo[1,5-*a*]pyrimidine-2-carbohydrazonoyl cyanide **(9a).**
Dark brown crystals; yield 80%; m.p. > 300 °C; IR (KBr) ν_{max} / cm^{-1} = 3426 (NH), 2218 (CN);^{1} H NMR

(DMSO) δ = 7.13-7.42 (m, 5H, Ar), 7.32-7.85 (m, 4H, Ar), 7.59-7.64 (m, 2H, thiophene), 8.06 (d, 1H , *J* = 4.5 Hz, thiophene),8.29 (s, 1H, pyrimidin), 11.45 (s, 1H, NH); ^{13}C NMR (DMSO) δ = 102.81, 111.63, 114.56, 116.38, 116.41, 116.71, 125.62, 128.49, 130.74, 133.85, 136.07, 139.10, 142.11, 149.31, 152.24, 155.20, 159.32, 160.55, 164.76; Anal. Calcd for $C_{25}H_{14}FN_7S$ (463.49): C, 64.79; H, 3.04; F, 4.10; N, 21.15; S, 6.92. Found: C, 64.65; H, 3.26; N, 21.26; S, 6.79%.

3-Cyano-7-(4-fluorophenyl)-5-(thiophen-2-yl)-*N*-(*p*-tolyl)pyrazolo[1,5-*a*]pyrimidine-2-carbohydrazonoyl cyanide **(9b).**
Dark brown crystals; yield 90%; m.p. > 300 °C; IR (KBr) ν_{max} / cm^{-1} = 3433 (NH), 2219 (CN); ^{1}H NMR (DMSO) δ = 2.54 (s, 3H, CH_3), 7.26-7.29 (m, 2H, thiophene), 7.34-7.85 (m, 4H, Ar), 7.58-7.61 (m, 4H, Ar), 8.14 (d, 1H , *J* = 4.4 Hz, thiophene), 8.39 (s, 1H,pyrimidin), 11.32 (s, 1H, NH); Anal. Calcd for $C_{26}H_{16}FN_7S$ (477.52): C, 65.40; H, 3.38; F, 3.98; N, 20.53; S, 6.71. Found: C, 65.55; H, 3.53; N, 20.67; S, 6.60%.

3-Cyano-7-(4-fluorophenyl)-*N*-(2-methoxyphenyl)-5-(thiophen-2-yl)pyrazolo[1,5-*a*]-pyrimidine-2-carbohydrazonoyl cyanide **(9c).**
Dark brown crystals; yield 90%; m.p. > 300 °C; IR (KBr) ν_{max} / cm^{-1} = 3425 (NH), 2213 (CN); ^{1}H NMR (DMSO) δ = 3.64 (s, 3H, OCH_3), 7.23-7.55 (m, 4H, Ar), 7.38-7.49 (m, 2H, thiophene), 7.82-7.86 (m, 4H, Ar), 8.05 (d, 1H , *J* = 4.5 Hz, thiophene), 8.26 (s, 1H, pyrimidin), 11.44 (s, 1H, NH); ^{13}C NMR (DMSO) δ = 58.41, 103.34, 110.59, 116.52, 116.94, 118.20, 122.35, 128.04, 130.11, 135.67, 139.43, 142.52, 146.43, 149.02, 152.11, 155.96, 159.21, 162.54, 165.71; Anal. Calcd for $C_{26}H_{16}FN_7OS$ (493.52): C, 63.28; H, 3.27; F, 3.85; N, 19.87; S, 6.50. Found: C, 63.43; H, 3.15; N, 19.74; S, 6.38%.

N-(2-Chloro-6-methylphenyl)-3-cyano-7-(4-fluorophenyl)-5-(thiophen-2-yl)pyrazolo[1,5-*a*]-pyrimidine-2-carbohydrazonoyl cyanide **(9d).**
Dark brown crystals; yield 69%; m.p. > 300 °C; IR (KBr) ν_{max} / cm^{-1} = 3431 (NH), 2214 (CN); ^{1}H NMR (DMSO) δ = 2.74 (s, 3H, OCH_3), 7.15-7.26 (m, 1H, Ar), 7.39-7.42 (m, 2H, thiophene), 7.45 (d, 2H, *J* = 8.5 Hz, Ar), 7.47- 7.86 (m, 4H, Ar), 8.01 (d, 1H , *J* = 4.5 Hz, thiophene), 8.20 (s, 1H, pyrimidin), 11.31 (s, 1H, NH); Anal. Calcd for $C_{26}H_{15}ClFN_7S$ (511.96): C, 61.00; H, 2.95; Cl, 6.92; F, 3.71; N, 19.15; S, 6.26. Found: C, 61.15; H, 2.81; N, 19.29; S, 6.13%.

N-(4-Chlorophenyl)-3-cyano-7-(4-fluorophenyl)-5-(thiophen-2-yl)pyrazolo[1,5-*a*]-pyrimidine-2-carbohydrazonoyl cyanide **(9e).**
Dark brown crystals; yield 90%; m.p. > 300 °C; IR (KBr) ν_{max} / cm^{-1} = 3428 (NH), 2211 (CN); ^{1}H NMR (DMSO) δ = 7.13-7.16 (m, 4H, Ar), 7-19-7.29 (m, 2H, thiophene), 7.37- 7.89 (m, 4H, Ar), 8.12 (d, 1H , *J* = 4.3 Hz, thiophene), 8.35 (s, 1H, pyrimidin), 11.28 (s, 1H, NH); Anal. Calcd for $C_{25}H_{13}ClFN_7S$ (497.94): C, 60.30; H, 2.63; Cl, 7.12; F, 3.82; N, 19.69; S, 6.44. Found: C, 60.45; H, 2.49; N, 19.54; S, 6.56%.

3-Cyano-7-(4-fluorophenyl)-5-(furan-2-yl)-*N*-phenylpyrazolo[1,5-*a*]pyrimidine-2-carbohydrazonoyl cyanide **(9f).**
Dark brown crystals; yield 90%; m.p. > 300 °C; IR (KBr) ν_{max} / cm^{-1} = 3421 (NH), 2214 (CN); ^{1}H NMR (DMSO) δ = 6.96-7.23 (m, 1H, furan), 7.03-7.29 (m, 5H, Ar), 7.47- 7.86 (m, 4H, Ar), 7.98 (d, 2H , *J* = 5 Hz, furan), 8.20 (s, 1H, pyrimidin), 11.31 (s, 1H, NH); Anal. Calcd for $C_{25}H_{14}FN_7O$ (447.43): C, 67.11; H, 3.15; F, 4.25; N, 21.91. Found: C, 67.27; H, 3.23; N, 21.85%.

3-Cyano-7-(4-fluorophenyl)-5-(furan-2-yl)-*N*-(*p*-tolyl)pyrazolo[1,5-*a*]pyrimidine-2-carbohydrazonoyl cyanide **(9g).**
Dark brown crystals; yield 78%; m.p. > 300 °C; IR (KBr) ν_{max} / cm^{-1} = 3430 (NH), 2217 (CN); ^{1}H NMR

(DMSO) δ = 2.43 (s, 3H, CH_3), 6.89- 6.94 (m, 1H, furan), 7.49-7.54 (m, 4H, Ar), 7.84-7.92 (m, 4H, Ar), 8.07(s, 1H, pyrimidin), 11.55 (s, 1H, NH); ^{13}C NMR (DMSO) δ = 26.71, 103.54, 106.10, 110.92, 116.48. 117.22, 129.28, 132.51, 134.60, 139.18, 142.55, 145.67, 149.11, 152.81, 155.93, 159.40, 160.31, 164.12, 165.32; Anal. Calcd for $C_{26}H_{16}FN_7O$ (461.46): C, 67.67; H, 3.49; F, 4.12; N, 21.25. Found: C, 67.54; H, 3.35; N, 21.39%.

3-Cyano-7-(4-fluorophenyl)-5-(furan-2-yl)-*N*-(2-methoxyphenyl)pyrazolo[1,5-*a*]pyrimidine-2-carbohydrazonoyl cyanide **(9h).**
Dark brown crystals; yield 92%; m.p. > 300 °C; IR (KBr) ν_{max} / cm^{-1} = 3421 (NH), 2212 (CN); ^{1}H NMR (DMSO) δ = 3.65 (s, 3H, OCH_3), 6.91-7.20 (m, 1H, furan), 7.29-7.42 (m, 4H, Ar), 7.45-7.84 (m, 4H, Ar), 7.93 (d, 2H , *J* = 5.2 Hz, furan), 8.32 (s, 1H, pyrimidin), 11.61 (s, 1H, NH); Anal. Calcd for: $C_{26}H_{16}FN_7O_2$ (477.46): C, 65.41; H, 3.38; F, 3.98; N, 20.54. Found: C, 65.56; H, 3.24; N, 20.30%.

N-(2-Chloro-6-methylphenyl)-3-cyano-7-(4-fluorophenyl)-5-(furan-2-yl)pyrazolo[1,5-*a*]-pyrimidine-2-carbohydrazonoyl cyanide **(9i).**
Dark brown crystals; yield 74%; m.p. > 300 °C; IR (KBr) ν_{max} / cm^{-1} = 3426 (NH), 2213 (CN); ^{1}H NMR (DMSO) δ = 2.37 (s, 3H, CH_3), 6.95-7.22 (m, 1H, furan), 7.20-7.32 (m, 1H, Ar), 7.31-7.65 (m, 2H, Ar), 7.79-7.84 (m, 4H, Ar), 7.89 (d, 2H , *J* = 5 Hz, furan), 8.17 (s, 1H, pyrimidin), 11.39 (s, 1H, NH); Anal. Calcd for $C_{26}H_{15}ClFN_7O$ (495.90): C, 62.97; H, 3.05; Cl, 7.15; F, 3.83; N, 19.77. Found: C, 62.82; H, 3.17; Cl, 7.28; N, 19.65%.

N-(4-Chlorophenyl)-3-cyano-5-(4-fluorophenyl)-7-(furan-2-yl)pyrazolo[1,5-*a*]pyrimidine-2-carbohydrazonoyl cyanide **(9j).**
Dark brown crystals; yield 91%; m.p. > 300 °C; IR (KBr) ν_{max} / cm^{-1} = 3434 (NH), 2218 (CN); ^{1}H NMR (DMSO) δ = 6.93-7.04 (m, 1H, furan), 7.24-7.27 (m, 4H, Ar), 7.35-7.87 (m, 4H, Ar), 7.93 (d, 2H , *J* = 5.2 Hz, furan), 8.08 (s, 1H, pyrimidin), 11.57 (s, 1H, NH); ^{13}C NMR (DMSO) δ = 102.24, 104.31, 116.42, 116.76. 117.55, 129.34, 134.71, 136.87, 139.32, 142.09, 147.17, 149.06, 152.12, 155.22, 159.76, 160.14, 164.90, 166.32 Anal. Calcd for $C_{25}H_{13}ClFN_7O$ (481.88): C, 62.31; H, 2.72; Cl, 7.36; F, 3.94; N, 20.35. Found: C, 62.46; H, 2.58; N, 20.49%.

Antimicrobial activity
Method of testing
The sterilized media was poured onto the sterilized Petri dishes (20-25) ml, each petri dish) and allowed to solidify at room temperature. Microbial suspension was prepared in sterilized saline equivalent to McFarland 0.5 standard solution (1.5x 10^5 CFU mL^{-1}) and its turbidity was adjusted to OD = 0.13 using spectrophotometer at 625 nm. Optimally, within 15 minutes after adjusting the turbidity of the inoculum suspension, a sterile cotton swab was dipped into the adjusted suspension and was flooded on the dried agar surface then allowed to dry for 15 minutes with lid in place. Wells of 6 mm diameter was made in the solidified media with the help of sterile borer. 100 µL of the solution of the tested compound was added to each well with the help of micropipette. The plates were incubated at 37 °C for 24 h in case of antibacterial activity. This experiment was carried out in triplicate and zones of inhibition were measured in mm. scale [22].

Anticancer activity
Materials and methods
Cell line
Human lung fibroblast cell line (WI-38), Hepatocellular carcinoma (HEPG2), Mammary gland breast cancer (MCF7) and Epithelioid Carcinoma (Hela). The cell lines were obtained from ATCC via Holding company for biological products and vaccines (VACSERA), Cairo, Egypt. Doxorubicin

was used as a standard anticancer drug for comparison.

Chemical reagents

The reagents RPMI-1640 medium, MTT and DMSO (sigma co., St. Louis, USA), Fetal Bovine serum (GIBCO, UK)

MTT assay

The cell lines mentioned above were used to determine the inhibitory effects of compounds on cell growth using the MTT assay. This colorimetric assay is based on the conversion of the yellow tetrazolium bromide (MTT) to a purple formazan derivative by mitochondrial succinate dehydrogenase in viable cells. Cell lines were cultured in RPMI-1640 medium with 10% fetal bovine serum. Antibiotics added were 100 units/ml penicillin and 100µg/ml streptomycin at 37 C in a 5% Co_2 incubator. The cell lines were seedes in a 96-well plate at a density of $1.0x10^4$ cells/well. at 37 C for 48 h under 5% Co_2. After incubation the cells were treated with different concentration of compounds and incubated for 24 h. After 24 h of drug treatment, 20 µl of MTT solution at 5mg/ml was added and incubated for 4 h. Dimethyl sulfoxide (DMSO) in volume of 100 µl is added into each well to dissolve the purple formazan formed. The colorimetric assay is measured and recorded at absorbance of 570 nm using a plate reader (EXL 800, USA). The relative cell viability in percentage was calculated as (A570 of treated samples/A570 of untreated sample) X 100 [23,24].

3. Results and Discussion

The reaction of starting 4-fluorobenzaldehyde (**1**) with each of 2-acetylthiophene (**2a**) and 2-acetylfuran (**2b**) under Claisen-Schmidt condensation route [25], in ethanol in the presence of 20% potassium hydroxide at room temperature yielded the corresponding *α,β*-unsaturated carbonyl compounds (chalcones) **3a,b** (Scheme 1). The structure of the **3a,b** was elucidated through their elemental analysis and spectra technique. As example, the IR spectrum of **3a** revealed a characteristic band at wavelength at 1644 cm^{-1} to carbonyl function. Also, a new C=C stretching group in the IR absorption band at 1590 cm^{-1} appeared. The ^{1}H NMR spectrum of **3a** exhibited two doublets at δ = 7.20 and 7.64 ppm referred to CH=CH protons, beside one multiplet signal at δ = 7.27 ppm corresponding to thiophene proton and two other multiplet signals at δ = (7.38-7.87) and (7.98-8.13) ppm for aromatic and thiophene protons, respectively.

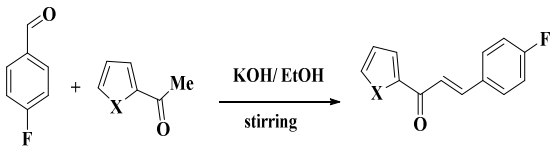

1 2a, X = S b, X= O 3a, X = S b, X= O

Scheme 1

Treatment of **3a,b** with 5-amino-3-cyanomethyl-1*H*-pyrazole-4-carbonitrile (**4**) in sodium ethoxide solution, the respective condensed products that were identified as pyrazolo[1,5-*a*]pyrimidine derivatives**5a,b** were obtained (Scheme 2). The IR spectrum of compound **5a**, taken as an example, showed a characteristic nitrile band at 2218 cm^{-1}. Also exhibited a singlet signal at δ 3.77 ppm due to the methylene protons along with pyrimidine-H at δ 8.29 ppm, besides the expected signals for aryl protons in its ^{1}H NMR chart. The formation of condensed products **5a,b** was assumed to proceed through the *Micheal*-type addition of the ring nitrogen in 5-amino pyrazole **4** (which is more active) to the activated double bond of **3a,b** followed by intramolecular cyclization with the elimination of water molecule and dehydrogenation [26,27]. The structures of the isolated compounds were

appropriately established by the spectroscopic and analytical methods.

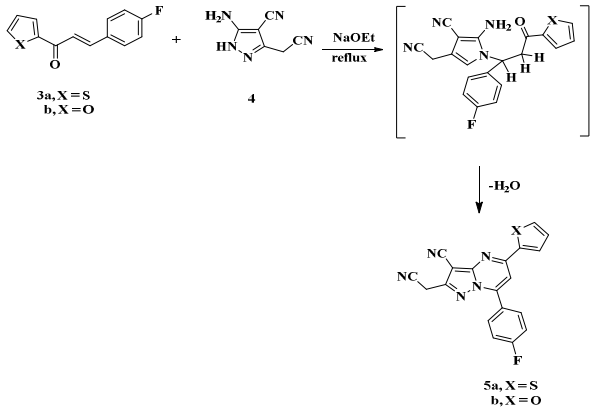

Scheme 2

Condensation of **5a,b** with different aldehydes in *N,N*-dimethylformamide with catalytic amount of piperidine formed the respective arylmethylene derivatives **7a-l** (Scheme 3). In the ^{1}H NMR spectrum of **7c**, the methylene protons at δ = 3.77 ppm was absent instead the two OCH_3`s protons appeared at δ = 3.65 and 3.72 ppm besides multiplet signals referred to aryl and vinylic signals at δ = 6.82-7.85 ppm. In addition to a doublet signal at δ = 7.92 with *J* coupling constants 5 Hz, along with a pyrimidine-H signal at 8.32 ppm. The IR spectrum for **7c** showed absorption band at wavelength 2213 cm^{-1} for nitrile function. There are significant signals in the ^{13}C NMR spectrum of **7c** at δ = 57.22, 59.62, 116.72, 116.94 and 140.35 for two C-OCH_3, two cyano groups and pyrimidine-carbon, respectively, with another expected signals. The spectral data together with elemental data agreed with the suggested structures **7a-l** (See exp. and Scheme 3).

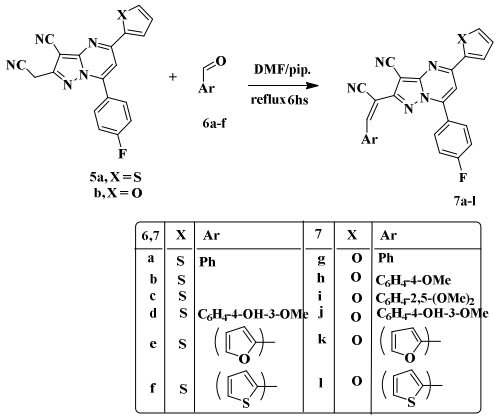

6,7	X	Ar	7	X	Ar
a	S	Ph	g	O	Ph
b	S		h	O	C_6H_4-4-OMe
c	S		i	O	C_6H_4-2,5-$(OMe)_2$
d	S	C_6H_4-4-OH-3-OMe	j	O	C_6H_4-4-OH-3-OMe
e	S		k	O	
f	S		l	O	

Scheme 3

Coupling of compounds **5a,b** with arene-diazonium salts **8a-e** (which prepared from diazotization of primary aromatic amine salts with sodium nitrite at 0-5 ^{o}C) in pyridine at 0-5 ^{o}C, afforded the arylhydrazo derivatives **9a-j** (Scheme 4). The structures of the latter products were established based on their elemental analysis and spectral data (See Experimental part). For example, the IR spectra of the products exhibited, in each case, the presence of one NH absorption band in the region 3425 cm^{-1}, besides nitriles absorption bands near to 2213 cm^{-1}. The ^{1}H NMR spectrum of compound **9c**, taken as a typical example of the prepared series, showed two singlet signals at δ 3.64 and 8.26 ppm to OCH_3`s and pyrimidine protons, respectively, beside the expected chemical shift, a D_2O-exchangable signal δ at 11.44 due to NH proton. Its ^{13}C NMR revealed the characteristic signals at 58.41, 116.52 and 116.94 due to methoxy, and nitrile carbons, respectively, besides the other expected signals.

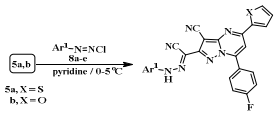

8,9	X	Ar^1	9	X	Ar^1
a	S	Ph	f	O	Ph
b	S	C_6H_4-4-Me	g	O	C_6H_4-4-Me
c	S	C_6H_4-2-OMe	h	O	C_6H_4-2-OMe
d	S	C_6H_4-6Cl-2-Me	i	O	C_6H_4-6-Cl-2-Me
e	S	C_6H_4-4-Cl	j	O	C_6H_4-4-Cl

(Scheme 4)

4. Biological activity

4.1. Antimicrobial activity:

The antimicrobial activity of tested compounds was determined using agar well diffusion method. All the compounds were tested *in vitro* for their antibacterial activity against *Staphylococcus aureus* and *Streptococcus mutans* (Gram positive bacteria), *Escherichia coli*, *Pseudomonas aeruginosa* and *Klebsiella pneumonia* (Gram negative bacteria) using nutrient agar medium. The antifungal activity of the tested compounds was tested against *Candida albicans* and *Asperagillus niger* using Sabouraud dextrose agar medium. Ampicillin and Gentamicin were used as standard drugs for Gram positive and Gram-negative bacteria, respectively. Nystatin was used as a standard drug for fungi strains. DMSO was used as solvent (negative) control. The compounds were tested at a concentration of 15 mg/ml against both bacterial and fungal strains. From results depicted in Table 1, we concluded all prepared compounds have no activity against all tested species of bacteria and fungi, but the target compounds **9a**,**b**, **9e** and **25h** exhibited moderate activity against staphylococcus aureus bacteria.

	Microorganism				
	Gram negative bacteria		**Gram positive bacteria**		**Fungi**
	Escherichia coli (ATCC:10536)	***Klebsiella pneumonia (ATCC:10031)***	***Staphylococcus aureus (ATCC:13565)***	***Streptococcus mutans (ATCC:25175)***	***Candida albicans (ATCC:10231)***
Standard Antibiotic	**Gentamicin**		**Ampicillin**		**Nystatin**
	27±0.5	**25±0.5**	**22±0.1**	**30±0.5**	**21±0.5**
Sample					
7a	**NA**	**NA**	**NA**	**NA**	**NA**
7b	**NA**	**NA**	**NA**	**NA**	**NA**
7c	**NA**	**NA**	**NA**	**NA**	**NA**
7d	**NA**	**NA**	**NA**	**NA**	**NA**
7e	**NA**	**NA**	**NA**	**NA**	**NA**

7f	**NA**	**NA**	**NA**	**NA**	**NA**
7g	**NA**	**NA**	**NA**	**NA**	**NA**
7h	**NA**	**NA**	**NA**	**NA**	**NA**
7i	**NA**	**NA**	**NA**	**NA**	**NA**
7j	**NA**	**NA**	**NA**	**NA**	**NA**
7k	**NA**	**NA**	**NA**	**NA**	**NA**
7l	**NA**	**NA**	**NA**	**NA**	**NA**
9a	**NA**	**NA**	**12.3±0.5**	**NA**	**NA**
9b	**NA**	**NA**	**12.6±0.5**	**NA**	**NA**
9c	**NA**	**NA**	**NA**	**NA**	**NA**
9d	**NA**	**NA**	**NA**	**NA**	**NA**
9e	**NA**	**NA**	**19.3±0.6**	**9.3±0.5**	**NA**
9f	**NA**	**NA**	**NA**	**NA**	**NA**
25g	**NA**	**NA**	**NA**	**NA**	**NA**
25h	**NA**	**NA**	**0.9±0.5**	**NA**	**NA**

Zone of inhibition is expressed in the form of Mean ± Standard deviation (mm).
NA: No activity.
Well diameter (6mm).
100µl was tested.

4.2. Anticancer activity

Cytotoxicity assay

In vitro anticancer evaluations

In order to determine the potential anticancer activity, the prepared compounds were tested for their in *vitro* cytotoxicity to the human hepatocarcinoma (HepG2) breast (MCF7), and cervical carcinoma (HeLa) cell lines using the MTT assay. Anticancer assay`s results varied from very strong to weak activity, however, the tested compounds have very strong to moderate activity with better IC_{50} values. In the series of **7a-l**, the compounds **7g** and **7h** showed moderate anticancer activity in the three cell lines compared to doxorubicin (Table 1). Compound **7k**, which containing heterocyclic (furan) moiety caused improvement in the anticancer activity among **7g** and **7h** in the HepG2, MCF7 and HeLa cell lines of IC_{50}

values 14.62 ± 1.2, 11.20 ± 0.9 and 10.04 ± 0.8 µM, respectively compared to doxorubicin (see Table 1).

Table 1. IC_{50} of compounds **7a-l** against three human cell lines with doxorubicin

Comp. no.	HePG2	MCF7	HeLa
DOX	4.50±0.2	4.17±0.2	5.57±0.4
7a	28.23±2.2	42.95±2.3	32.75±2.2
7b	82.17±4.3	78.12±3.8	73.50±3.8
7c	56.60±3.2	72.58±3.6	64.27±3.5
7d	62.34±3.5	68.01±3.4	47.36±2.7
7e	67.25±3.8	53.29±2.9	60.14±3.2
7f	51.03±3.1	48.67±2.6	39.26±2.4
7g	24.53±2.0	29.27±1.9	15.83±1.2
7h	37.82±2.5	31.59±2.1	26.19±1.9
7i	7.84±0.6	5.63±0.4	3.71±0.1
7j	9.91±0.8	8.16±0.6	6.29±0.3
7k	14.62±1.2	11.20±0.9	10.04±0.8
7l	19.10±1.5	23.46±1.7	17.83±1.4

Introduction of methoxy and hydroxyl moieties in phenyl core as in case **7j**, increased the activity to give very strong anticancer agent with IC_{50} = 9.91 ± 0.8, 8.16 ± 0.6 and 6.29 ± 0.3 µM 7µM in HepG2, MCF7 and HeLa cell lines, respectively. While, the highest activity was attained by introducing two methoxy groups in phenyl ring as in case **7i** with IC_{50} values 7.84 ± 0.6, 5.63 ± 0.4 and 3.71 ± 0.1 µM in HepG2, MCF7 and HeLa cell lines, respectively. The other tested compounds of this series showed weak activity against the tested three cell lines. In the series **9a-c** and **9f-h** exhibited moderate to weak activity except the compound **9b** showed strong activity in the three cell lines with IC_{50} = 14.53 ± 1.2, 10.86 ± 0.8 and 27.90 ± 2.1 µM in HepG2, MCF7, and HeLa, respectively.

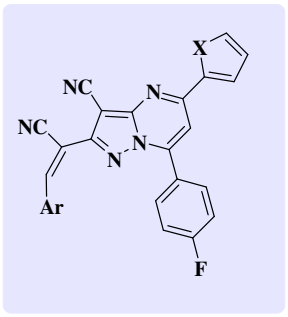

7a-I

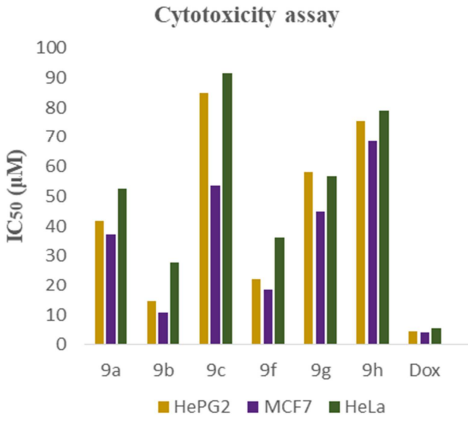

Fig. 3: Revealing IC_{50} of **7a-l** against HePG2, MCF7 and HeLa cell lines compared to doxorubicin

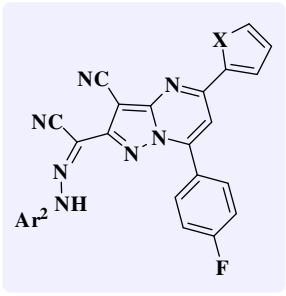

9a-h

Table 2. IC_{50} of compounds **9a-c** and **9f-h** against three human cell lines with doxorubicin

Comp. no.	HePG2	MCF7	HeLa
DOX	4.50±0.2	4.17±0.2	5.57±0.4
9a	41.87±2.6	37.34±2.4	52.36±3.1
9b	14.53±1.2	10.86±0.8	27.90±2.1
9c	84.76±4.1	53.41±3.1	91.63±4.9
9f	22.19±1.9	18.30±1.5	36.18±2.5
9g	58.10±3.4	44.93±2.8	56.57±3.3
9h	75.62±3.9	68.62±3.6	79.02±3.8

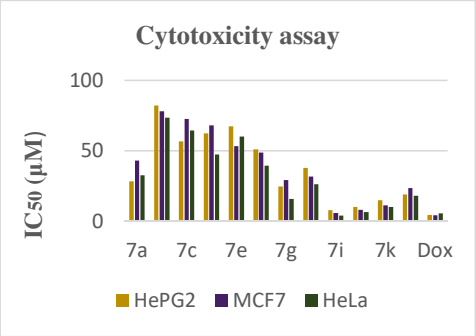

Fig. 4. Revealing IC_{50} of **9a-c** and **9f-h** against HePG2, MCF7 and HeLa cell lines compared to doxorubicin

4.3. In Vitro Cellular viability

Compounds **7i**, **7j**, **7k**, and **9b** were tested for cell viability against WI38 (human lung fibroblast cell line) using the MTT assay. The data shown in Table 3 indicate that the compound **7i**, which has the highest anticancer activity in the three cell lines, moderate cell viability in WI38 with IC_{50} = 41.26 ± 2.6 µM, which is weaker than that of compound **7j** with IC_{50} = 52.80 ± 3.0 µM, that occupied the second order in the cytotoxic activity and stronger than **7k** with IC_{50} = 36.38 ± 2.3 µM, which has the moderate cytotoxic activity. On the other hand, compound **9b** showed the highest cell viability among the other tested compounds with IC_{50} = 87.39 ± 4.4 µM.

Table 3: IC_{50} of compounds against human lung fibroblast cell line WI38

Comp. no.	Cell line (WI38) IC_{50} (µM)
7i	41.26 ± 2.6
7j	52.80 ± 3.0
7k	36.38 ± 2.3
9b	82.39 ± 4.4
Doxorubicin	6.72± 0.5

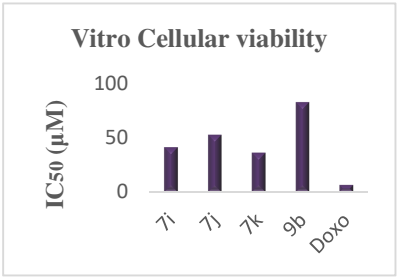

Fig. 5: Revealing IC_{50} of most potent compounds against human lung fibroblast cell line WI38

4.4. Molecular Docking Study

It have been reported that pyrazolo[1,5-*a*]pyrimidines effective inhibitors of cyclin-dependent kinases (CDKs) such as CDK1, CDK2 and others [28, 29], thus we used the crystal structure of human CDK2 [PDB: 1Y8Y]. For protein-ligand interaction stimulations, molecular docking was utilized for more potent anticancer agents **7i, 7j, 7k** and **9b** in addition to doxorubicin with the crystal structure [PDB: 1Y8Y] using the Molecular Operating

Environment (MOE 2015.10q) software to find the possible binding modes for the selected compounds.

The active site of 1Y8Y is self-docked, which showed two interactions, one hydrogen bond between nitrogen of pyrimidine moiety and amino acid Lys 129 with bond length 2.98 and 2.87 Å, along with arene-H between pyrazole ring and Gly 13 (Fig. 5). The active site of 1Y8Y interaction has binding energy (S) equals -6.2068 Kcal/mol and rmsd fine equals 1.7904. This value represents the average distance between the atoms and the original ligand. Compounds **7i**, **7j**, **7k**, and **9b** were docked with the CDK2, PDB [1Y8Y].

The ligand interaction pattern of most of the docked compounds showed common interactions with the amino acid residue Lys 129, Gly 13, Glu 8, Ile 10, Asp 89, Lys 33, and Lys 89. In the protein-ligand pattern, compounds **7i**, **7j**, **7k** and **9b** form hydrogen bonds through the cyano moiety of the pyrazole ring with the amino acids Lys 89, Asp 89, Lys 89 and Lys 33 with the bond lengths equal 3.80, 2.95, 3.80, and 3.60 Å, respectively, in contrast, compound **7j** forms another hydrogen bond between hydroxyl group in the phenyl ring and Glu 8 with bond length equal 2.97 Å. Also, in compound **7k** appeared an arene-H interaction between pyrimidine moiety and Ile 10. In addition, compound **7j** containing an arene-H bond between phenyl ring and Ile 10. The compounds **7i**, **7j**, **7k**, and **9b** are the most active compounds showing better IC_{50} values in the three cell lines, HePG2, MCF7, and HeLa. All of these compounds showed good interaction with the binding site as shown in Table 4 and figures 5-9. Compound **7i** showed a binding energy with the active site of 1Y8Y equals -6.5674 Kcal/mol and rmsd-fine equals 1.4246 with the formation of one hydrogen bond (Fig. 6). Similarly, compound **7j** interacted with the active site of 1Y8Y by the formation of two hydrogen bonds and one hydrogen-pi bond with S value equals -7.1674 Kcal/mol and rmsd-fine equals 2.080 (Fig. 7). The protein-ligand pattern of **7k** involved the formation of one hydrogen bond and a binding energy equals -7.3197 Kcal/mol and rmsd-fine 1.6759 (Fig. 8). Moreover, compound **9b** revealed the formation of one hydrogen bond with S equals -6.2582 Kcal/mol and rmsd-fine 2.0250 (Fig. 9). From the interaction patterns of all the compounds, we concluded that the presence of nitrile, and hydroxyl groups is important for the interactions with the active site pocket of 1Y8Y (see Table 4).

Table 4: Compounds and doxorubicin protein-ligand interactions with 1Y8Y, revealing the binding energy (S) and the amino acids involved in the interactions for the docked compounds

Compd no.	S Kcal/mol	Rmsd -fine	Amino acids contributed in the interaction	Length of bonds Å
1Y8Y	-6.2068	1.7904	Lys 129 Gly 13	H-Bond 2.98 Å (N-pyrimidine) Arene-H (pyrazole)
7i	-6.5674	1.4246	Lys 89	H-Bond 3.80 Å (CN)
7j	-7.1674	2.080	Gly 8 Asp 89 Ile 10	H-Bond 2.97 Å (OH) H-Bond 2.95 Å (CN) Arene-H (phenyl)
7k	-7.3197	1.6759	Lys 33 Ile 10	H-Bond 3.60 Å (CN) Arene-H (pyrimidine)
9b	-6.2582	2.0250	Lys 89	H-Bond 3.80 Å (CN)

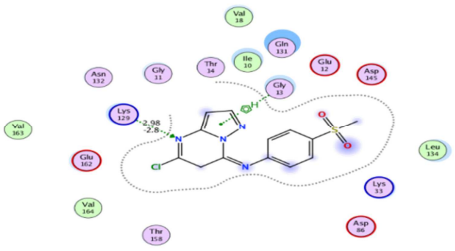

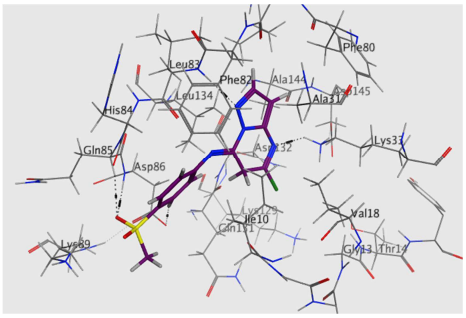

Fig. 5. Revealing the interactions of the active site of **1Y8Y** in 2D and 3D dimension

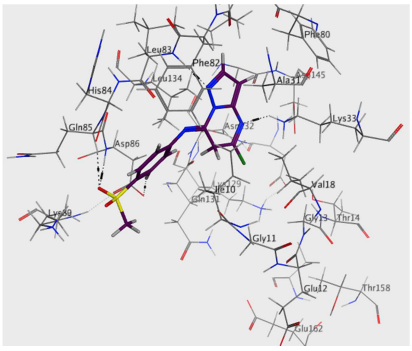

Fig. 7. Revealing the interactions of the active site of **1Y8Y** with **7j** in 2D and 3D structures

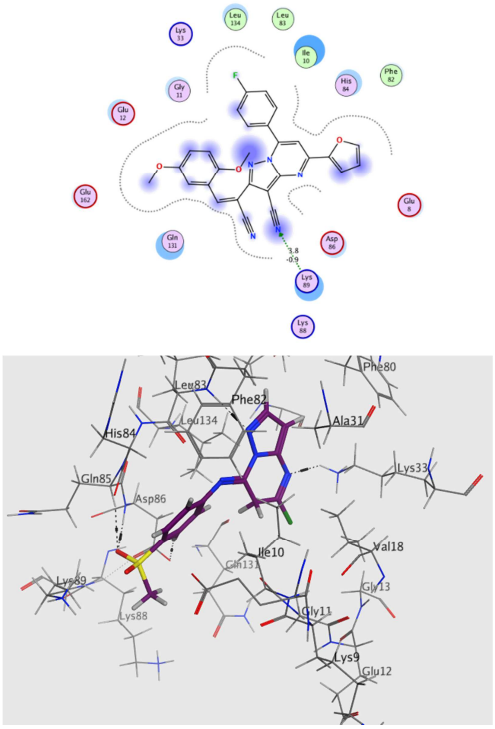

Fig. 6. Showing the interactions of the active site of **1Y8Y** with **7i** in 2D and 3D dimension

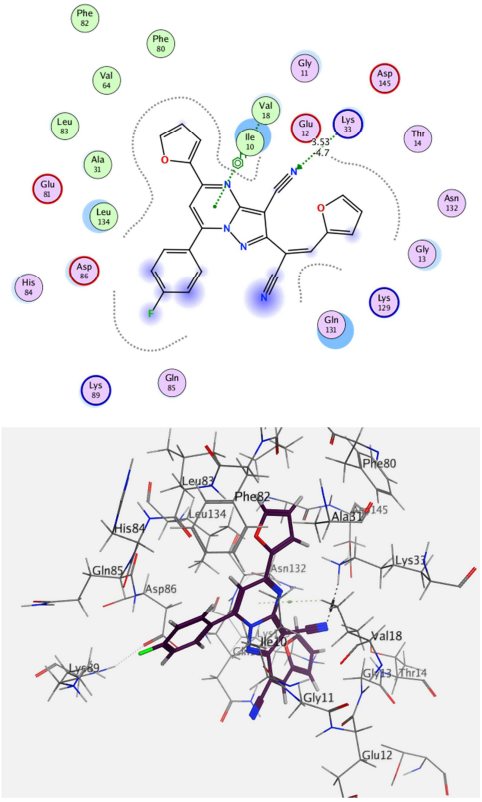

Fig. 8. Revealing the interactions of the active site of **1Y8Y** with **7k** in 2 and 3D structures

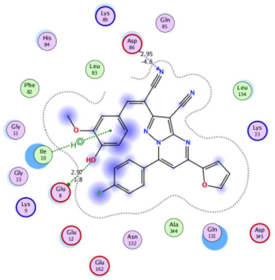

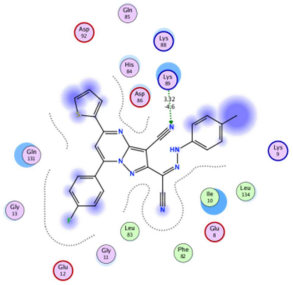

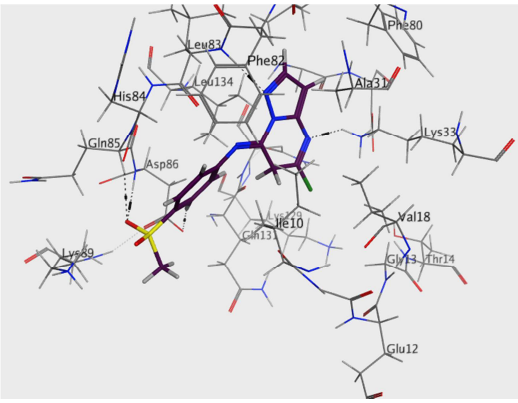

Fig. 9. Revealing the interactions of the active site of **1Y8Y** with **9b** in 2 and 3D dimention

4.5. In silico ADME study

The most potent cytotoxic compounds **7i**, **7j**, **7k** and **9b** were studied online using Swiss ADME (absorption, distribution, metabolism and excretion) to show the pharmacokinetic characters for them. From its study we predict that all tested compounds **7i, 7j, 7k** and **9b** exhibited low gastrointestinal absorption (white region) and no blood brain absorption (yellow region) as showed in boiled egg chart (Fig. 10). Additionally, compound **7i** and **7j** inhibit each of CYP2C9 and CYP3A4, in addition to **7j** acts as P-gp substrate. Also, compound **7k** inhibits CYP1A2, CYP2C9 and CYP3A4, but the azo derivative **9b** inhibits CYP2C9 (Table 5).

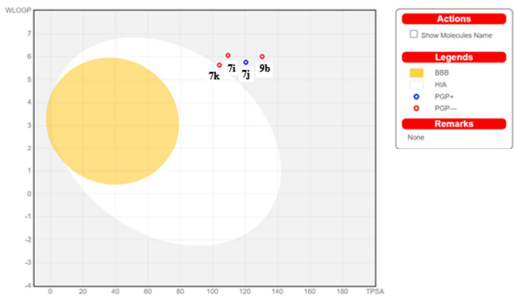

Fig 10. Boiled egg chart showed gastrointestinal absorption and blood brain penetration of compounds **7i, 7j, 7k** and **9k**

Table 5. In silico pharmacokinetic parameter of compounds **7i, 7j, 7k** and **9b**

parameter	7i	7j	7k	9b
GIA	Low	Low	Low	Low
BBB	NO	NO	NO	NO
P-gP substrate	NO	Yes	NO	NO
CYP1A2 inhibitor	NO	NO	Yes	NO
CYP2C9 inhibitor	Yes	Yes	Yes	Yes
CYP3A4 inhibitor	Yes	Yes	Yes	NO

GIA: Gastrointestinal absorption
BBB: Blood brain barrier
PgP: P-glyco protein transport
CYP1A2, CYP2C9 and CYP3A4: isoforms of CYP450

Drug likeness prediction of compounds **7i, 7j, 7k** and **9b** clarified that they obey Lipinski's rule where MWt ≤ 500, number of H bond donors ≤ 5, number of H bond acceptors ≤ 10, calculated logP ≤ 5 and TPSA ≤ 140 as showed in Table 6.

Table 6. Lipinisk's Parameters

Comp. no.	TPSA (Å²)	Log P	MWt	nHBD	nHBA	No. of viol.
7i	109.37	4.34	491.47	0	8	0
7j	129.24	3.52	477.45	1	8	0
7k	112.99	3.61	421.38	0	7	0
9	133.41	3.43	477.52	1	6	0

References

[1] Michael D., Embelin and Its Derivatives: Design,Synthesis and Potential Delivery Systems for Cancer Therapy, *Pharmaceuticals (Basel)*, **15** (9), 1131 (2022).

[2] Andres A.G., Andrés G., and Jaime P., Functional Pyrazolo[1,5-*a*]pyrimidines: Current Approaches in Synthetic Transformations and Uses As an Antitumor Scaffold, *Molecules*, **26** (9), 2708 (2021).

[3] Yongjie Z. , Yan L. , Ying Z. , Qing Z. , Tianfu H., Chunlei T. , Weizheng F., Pyrazolo[1,5-*a*]pyrimidine Based Trk Inhibitors: Design, Synthesis, Biological Activity Evaluation, *Bioorg Med Chem Lett*., **31**, 127712 (2021).

[4] Oh S., Libardo M. D. J., Shaik A., Pauly G.T, Roma J. S. O., Andaleeb S., Yoshitaka T., Caroline D., Michael G., Thomas R. I., Paul G. W., Ray P. C., Gray D. W. , Boshoff H.I. M., and Barry C.E., Structure-Activity Relationships of Pyrazolo[1,5-*a*]pyrimidin7(4*H*)-ones as Antitubercular Agents, *ACS Infectious Diseases*, ***7*** (2), 479-492 (2021).

[5] Johansson N. G. , Loïc D., Dr. Keni V., Dr. Ayman K., Jianing L., Arthur L., Dr. Orquidea R., Dr. Alexandros K., Dr. Gustav B. G., Prof. Seppo M., Prof. Adrian G., Prof. Jari Y., Dr. Henri X., Exploration of Pyrazolo[1,5-*a*]pyrimidines as Membrane-Bound Pyrophosphatase Inhibitors, *ChemMedChem* , **16**, 3360-3367 (2021).

[6] Varma R. R., Pandya J. G., Vaidya F. U., Chandramani P., Bhatt 1 B. S. and Patel1 M.N., Synthesis, Characterization and Biological Application of Pyrazolo[1,5-*a*]pyrimidine Based Organometallic Re(I) Complexes, *Acta Chim. Slov*, **67**, 957–969 (2020).

[7] Kamil P., Dwyer M.P. , Carmen A., Courtney B., Tin-Yau C., Doll R. J., Kerry K., Chad K., Brian M., Jocelyn R., Randall R., Greg T., Thierry F., Alan H., Vincent M., Amin A. N., Yaolin W., Paul K., Emma L., David P., Nicole S., Wolfgang S., Lesley S., Frances S., Derek W., Xiaoying X., Quiao Z., James R. A., Paradkar V. M., Haengsoon P., Rokosz L. R., StauffeT. M. R, and Timothy J. G., Discovery of Dinaciclib (SCH 727965): A Potent and Selective Inhibitor of Cyclin-Dependent Kinases, *ACS Med Chem Lett*., **1**(5): 204–208 (2010).

[8] Ajeesh K. A.K. , Bodke Y. D. , Peter S. L., Ganesh S. & Bhat K. G., Design, Synthesis and Anti-cancer Evaluation of a Novel Series of Pyrazolo [1,5-*a*] pyrimidine Substituted Diamide derivatives, *Medicinal ChemistryResearch* , **26**, 714–744 (2017).

[9] Nagano T., Tachihara M., Dacomitinib Y. N., A Second-generation Irreversible Epidermal Growth Factor Receptor Tyrosine Kinase Inhibitor (EGFR-TKI) to Treat Non-small Cell Lung Cancer, *Drugs Today (Barc)*, **55**, 231-236 (2019).

[10] Metwally N. H., Deeb E. A., Synthesis, Anticancer Assessment on Human Breast, Liver and Colon Carcinoma Cell Lines and Molecular Modeling Study Using Novel Pyrazolo[4,3-*c*]pyridine derivatives, *Bioorg. Chem*., **77**, 203-214 (2018).

[11] Metwally N. H., Badawy M. A., Okpy D. S., Green Synthesis of Some New Thiopyrano[2,3-*d*]thiazolo][1,3]thiazoles using Lemon Juice and Their Antibacterial Activity, *Synth. Commun*. **48**, 2496-2509 (2018).

[12] Metwally N. H., Mohamed S. M., Ragb E. A., Design, Synthesis, Anticancer Evaluation, Molecular Docking and Cell Cycle Analysis of 3-Methyl-4,7-dihydropyrazolo[1,5-*a*]pyrimidine derivatives as Potent Histone Lysine Demethylases (KDM) Inhibitors and Apoptosis Inducers, *Bioorg. Chem*., **88**, 1029299 (2019).

[13] Metwally N. H., Saad G. R., Abdwahab E. A.,Grafting of Multiwalled Carbon Nanotubes with Pyrazole derivatives: Characterization, Antimicrobial Activity and Molecular Docking Study, *Int. J. Nanomed*., **20**, 6645-6659 (2019).

[14] Metwally N. H., Mohamed M. S., New Imidazolone derivatives Comprising a Benzoate or Sulfonamide Moiety as Anti-inflammatory and Antibacterial Inhibitors: Design, Synthesis, Selective COX-2, DHFR and Molecular-modeling Study, *Bioorg. Chem*., **99**, 103438 (2020).

[15] Metwally N. H., Abdallah S. O., Mohsen M. M., Design, Green One-pot Synthesis and Molecular Docking Sstudy of Novel *N*,*N*-bis(cyanoacetyl) Hydrazines and Bis-coumarins as Effective Inhibitors of DNA Gyrase and Topoisomerase IV, *Bioorg.Chem*., **97**, 103672 (2020).

[16] Metwally N. H., Mohamed M. S., Deeb E. A., Synthesis, Anticancer Evaluation, CDK2 Inhibition, and Apoptotic Activity Assessment with Molecular Docking Modeling of New Class of Pyrazolo[1,5-*a*]pyrimidines, *Res. on Chem. Intermed*. , **47**, 5027-5060 (2021).

[17] Metwally N. H., Abd-Elmoety A. S., Novel Fluorinated Pyrazolo[1,5-*a*]pyrimidines: In a Way From Synthesis and Docking Studies to Biological Evaluation. *J. Molecular Str*.**1257**,132590 (2022).

[18] Metwally N. H., Badawy M. A., Okpy D. S., Synthesis, Biological Evaluation of Novel Thiopyrano[2,3-*d*]thiazoles Incorporating Arylsulfonate Moiety as Potential Inhibitors of Tubulin Polymerization, and Molecular Modelling Studies, *J. Mol. Str*., **1258**, 132848 (2022).

[19] Metwally N. H., El-gemeie G. H., Fahmy F. G., Green synthesis: Antimicrobial activity of novel

benzothiazole-bearing coumarin derivatives and their fluorescence properties, *Egypt. J of Chem.,* **65**, 679 (2022).

[20] Bhat K.I., Chauhan M.K.S., Kumar A., Kumar P., Synthesis, Pharmacological, and Biological Screening of Novel derivatives of Benzodiazepines, *Journal of Heterocyclic Chemistry*, **51** (4), 1189-1192 (2014).

[21]Pallavi H. M. Fares, HezamAl-Ostoot[ab]H., KameshwarVivek[c,] S.A., Synthesis, Characterization, DFT, Docking Studies and Molecular Dynamics of Some 3-phenyl-5-furan Isoxazole derivatives as Anti-inflammatory and Anti-ulcer agents, *Journal of Molecular Structure*, **1250**, 131812 (2022).

[22] Collee J. G., Duguid J. P., Fraser A. G., and Marmion B. P. (ed.), Laboratory Control of Antimicrobial Therapy, Mackie & McCartney-practical Medical Microbiology, *Scott, A. C* ., **13th ed**., 161-181 (1989).

[23] Mosmann T., Immunol J., *Methods*, **65**, 55-63 (1983).

[24] Denizot F., Lang R., Immunol J., *Methods*, **22**, 271-277 (1986).

[25] Dawane B. S.; Konda S. G., Shaikh B. M, Bhosale R. B., *Acta Pharm*., **59**, 473-482 (2009). 26] Ammar Y. A., El-Sharief A. M., Zahran M. A. Sh., ElSaid M. Z., El-Said V. H. J., *Chem Res*., **7**, 324 (1995).

[27] El-Gaby M. S. A., Sayed A. Z.; Abu-Shanab, F. A.; Hessein, A. M., *Phosphorus Sulfur Silicon*, **164**, 1 (2000).

[28] Galons H., Oumata N., Meijer L., *Exp. Opin. Ther. Pat*., **20**, 377 (2010)

[29] Williamson D.S., Parratt M.J., Bower J.F., Moore J.D., Richardson C.M., Dokurno P., Cansfield A.D., Francis G.L., Hebdon R.J., Howes R., Jackson P.S., Ockie A.M., Murray J.B., Nunns C.L., Powles J., Robertson A., Surgenor A.E., Torrance C.J., *Bioorg. Med. Chem. Lett*., **15**, 863 (2005).